JP Journal of Heat and Mass Transfer

https://pphmjopenaccess.com
https://doi.org/10.17654/0973576325016
Volume 38, Number 3, June 2025, Pages 315-339
P-ISSN: 0973-5763
E-ISSN: 3049-2556

EFFECTS OF RADIATION AND HEAT GENERATION ON MHD CASSON FLUID FLOWING IN A POROUS MEDIUM ROTATING ON AN INCLINED OSCILLATING VERTICAL PLATE

R. Raju[1], A. Selvaraj[1,*], S. Dilip Jose[2] and K. Chithra[3]

[1]Department of Mathematics
Vels Institute of Science, Technology and Advanced Studies
Chennai, 600117, Tamil Nadu, India

[2]Department of Mathematics
Periyar Maniammai Institute of Science and Technology
(Deemed to be University)
Vallam, Thanjavur, 613403, Tamil Nadu, India

[3]Department of Mathematics
Government Arts and Science College
Kallakurichi, 606202, Tamil Nadu, India

Received: September 29, 2024; Revised: January 28, 2025; Accepted: April 10, 2025

Keywords and phrases: MHD Casson fluid, porous medium, radiation effects, heat generation, inclined vertical plate, oscillating boundary.

*Corresponding author

Communicated by K. K. Azad

How to cite this article: R. Raju, A. Selvaraj, S. Dilip Jose and K. Chithra, Effects of radiation and heat generation on MHD Casson fluid flowing in a porous medium rotating on an inclined oscillating vertical plate, JP Journal of Heat and Mass Transfer 38(3) (2025), 315-339. https://doi.org/10.17654/0973576325016

Published Online: June 9, 2025

Abstract

A mathematical model of the unstable natural convective magnetohydrodynamic boundary layer flow of Casson fluid near an inclined oscillating perpendicular plate in a rotating porous medium has been studied. The field is uniformly transverse. The study incorporates heat production, absorption, and thermal emission and aims to accurately solve the prevailing non-dimensional partial differential equations using the Laplace transform method. The analysis focuses on key parameters like the magnetic field (M), heat absorption (Q), permeability (K), Prandtl number (P_r), Schmidt number (S_c), thermal radiation (R), Casson fluid parameter, Grashof numbers $(G_r$ and $G_c)$, permeation time (t), and porous medium parameter (K). These attributes encompass the influence of quickness, thermal conditions, and concentration profiles. An increase in the Casson fluid parameter and other Grashof parameters results in elevated velocity values. Regarding the magnetic field characteristic, a reversal in the trend has been noted. Results would ideally be optimally configured for application specific needs such as oil recovery and industrial cooling. It can be sensible to work with complex geometries, non-linear effects, and transient behavior to arrive at simulations that more accurately reflect real-life scenarios in these applications.

Nomenclature

x', y'	Cartesian coordinates (m)
u, v	Velocity components along x' and y' axes (m/s)
t	Time (s)
T	Temperature
T_w	Plate surface temperature
T_∞	Ambient temperature
C	Concentration (kg/m^3)

C_w Plate surface concentration (kg/m^3)

C_∞ Ambient concentration (kg/m^3)

μ Dynamic viscosity (Pa·s)

κ Thermal conductivity (W/m·K)

q' Complex velocity (m/s)

g Gravitational acceleration (m/s^2)

K Permeability of the porous medium (m^2)

M Magnetic parameter

P_r Prandtl number

S_c Schmidt number

G_r Thermal Grashof number

G_c Solutal Grashof number

Q Heat generation parameter

R Radiation parameter

ϕ Oscillation frequency

Greek Symbols

ρ Density (kg/m^3)

β Thermal expansion coefficient (K^{-1})

β^* Solutal expansion coefficient (kg/m^3)

σ^* Stefan-Boltzmann constant (W/m^2·K^4)

a^* Mean absorption coefficient (m^{-1})

ν Kinematic viscosity (m^2/s)

θ Dimensionless temperature

γ Casson fluid parameter

Subscripts

w	Plate surface
∞	Free stream or ambient conditions
0	Initial value

1. Introduction

Investigations into MHD movement processes with Casson fluids through porous materials, especially when forced into oscillatory motion, have great importance in engineering and biology. The Casson fluid is a subclass of non-Newtonian fluids that can behave as either solids or liquids, depending on the shear stress: at low shear stress, they behave like solids and like liquids at high shear stress. These unique features are of particular interest in the fields of lubricants, polymer processing, and blood flow dynamics, among others. This study deals with the flow of Casson fluid through a porous medium subjected to oscillations with a perpendicular incline plate underneath the effect of rotation and magnetic fields, emphasizing the effects of radiation and heat generation. Internal factors, including the tilt, oscillations, and rotation of the plate, interact to influence the temperature and velocity profiles. Bearing in mind radiation with heat-generating processes in terms of flow properties is crucial for the design of thermal stability and management systems. The work leads to advances in heat exchange understanding in biological and industrial systems involved in controlling the motion of non-Newtonian fluids and heat under magnetic field conditions. The literature review elaborated on heat transfer, chemical reactions, radiation, and boundary conditions upon the magnetohydrodynamic (MHD) movement of Casson fluids. Amar et al. [1] investigated the magnetohydrodynamic heat transfer flow of Casson fluid in a thermally active moving wedge concerning radiation and viscous dissipation. Arthur et al. [2] studied the flow of Casson fluid past a porous surface perpendicular to the direction of flow under the influence of chemical reactions and a magnetic field. Selvaraj and Jothi [3] studied fluid flow past a uniformly accelerated vertical plate with heat

sources on magnetohydrodynamics and radiation absorption. Bhavana et al. [4] examined the Soret effect for free convective unsteady magnetohydrodynamic flow heated from above by a flat plate. Yanala et al. [5] studied the instability of such magneto-Casson nanofluid flow, coupled with radiation, chemical reactions, and the non-linear stretching of the Riga plate. Devi and Anjali Raj [6] worked on the effects of thermo diffusion on heat and mass transfer within the scope of hydromagnetic free convective flows past a non-parallel sliding plate under thermal-slip conditions. Dilip Jose and Selvaraj [7] focused on parabolic flow across a fast isothermal vertical plate under the effects of rotation on convective heat and mass transfer. Maran et al. [8] looked at the effect of a first-order chemical reaction on magnetohydrodynamic flow over an infinitely thin perpendicular plate, satisfying variable mass diffusion and heat radiation. Kataria and Patel [9] studied chemical reactions and heat generation/absorption in superheated Casson flow across an exponentially accelerated plate. Hartmann [10] made a significant contribution to the flow induced by a magnetic field in relation to the hydrodynamics of electrically conducting fluids. Jamil et al. [11] studied how heat radiation affects slanted blood vessels that are exposed to the flow of magnetohydrodynamic (MHD) Casson fluid. In 2016, Kataria and Patel [12] explored the movement of Casson fluid over a reciprocating plate, emphasizing Soret diffusion and heat generation effects. McGregor [13] investigated the application of minimal energy principles within Casson fluid systems. Mernone et al. [14] performed a mathematical assessment related to peristaltic transport in these fluids. Mohan et al. [15] examined how radiation absorption and the Dufour effect influence unstable magnetohydrodynamic free convection in flows involving Casson fluids. Nandhini et al. [16] evaluated the relationship between radiation absorption and exponential parameters in chemically reactive Casson fluid traveling along an exponentially expanding sheet. Raghunatha et al. [17] focused on magnetohydrodynamics as it pertains to unstable flowing Casson fluids with internal heat sources present. Dilip Jose and Selvaraj [18] looked into parabolic flow dynamics regarding heat and mass diffusion under rotation, enhancing our comprehension of these phenomena in such systems. Finally, Selvaraj et al. [19] broadened their research to incorporate MHD effects

while Sindhu et al. [20] examined how rotation influences parabolic flow by focusing on temperature fluctuations and uniformity in mass distribution. Jothi et al. [21] attempted to obtain an idea about the changes of temperature and concentration in fluid dynamics due to combined effects of radiation absorption and magnetohydrodynamics near an exponentially accelerating perpendicular plate. Dilip Jose et al. [22], on the other hand, explored the parabolic flow in MHD due to temperature variations with mass diffusion. The studies by Jose et al. and Lakshmikaanth et al. [23, 24] explored the effects of chemical reactions, Hall currents, and heat sources on flow dynamics. Lakshmikaanth et al. [25] also discussed the interaction of radiation and chemical processes in parabolically fast flows. Aruna et al. [26] discussed the rotating fluids on MHD parabolic flow in the absence of current due to Hall and Dufour effects, and expanded knowledge of fluid behavior. This research uniquely concentrated on the combined effects of radiation and heat production on the MHD Casson fluid flow through a porous media rotating on an inclined plate that oscillates perpendicularly. This study represents the first comprehensive data compilation on this system, based on the authors' analysis and perspective. The magnetic field effects on the temperature and velocity field of the fluid have been analyzed, depending on angular speeds, oscillation frequency, and inclination angle. Integration of the study in relation to radiation and heat-generating species into Casson fluid systems demonstrates an advancement in development that gives rise to industrial, biological, and environmental technologies.

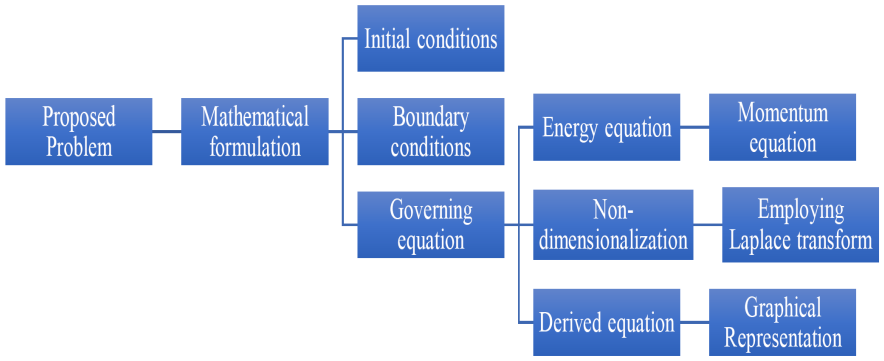

Figure 1. Flow chart of the proposed problem.

2. The Mathematical Formulation

Let us examine the Casson fluid stream in a porous media passing through an infinite vertical plate. Here we consider x'-axis to be "taken along the plate upward direction to the fluid flow and y'-axis taken normal direction towards the plate. A uniform magnetic field (B) of strength B_0 is used on an electrically conducting fluid perpendicular to the plate. The plate and fluid are initially at rest at time $t' \leq 0$, and kept at a uniform temperature T'_∞ and uniform surface concentration C'_∞. At time $t' \geq 0$, the plate is subjected to an oscillatory motion in the vertical direction, opposite to the gravitational field, with a velocity given by $u_0 \cos wt$. Simultaneously, heat transfer is initiated from the plate, where the plate temperature is varied linearly with time as to $T'_\infty + (T'_w - T'_\infty)\frac{t'}{t_0}$ for $t' \geq 0$, until it reaches a constant wall temperature T'_w. Similarly, the plate concentration is either increased or decreased linearly with time as $C'_\infty + (C'_w - C'_\infty)\frac{t'}{t_0}$ for $t' \geq 0$, until it reaches a constant concentration C'_w. It is supposed that the energy equation will not take into account the rigid plate, 1D flow, incompressible flow, viscous dissipation, as well as free convection factor.

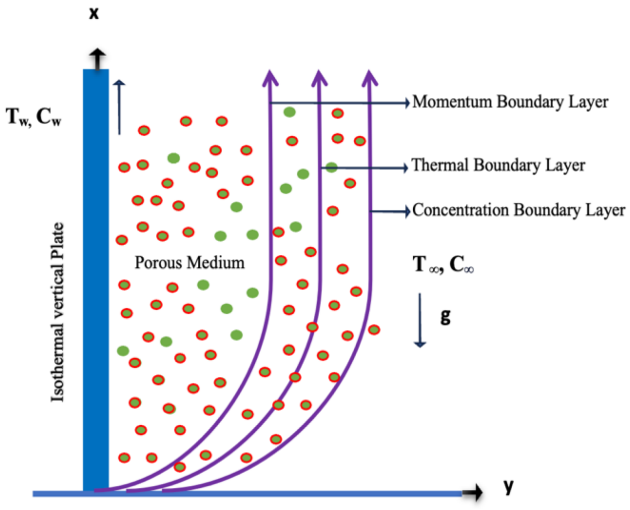

Figure 2. Geometry of the problem.

The governing partial differential equations with initial and boundary conditions are as follows, with the aforementioned assumptions and accounting for Boussinesq's approximation:

$$\frac{\partial u'}{\partial t'} - 2\Omega' v' = \nu\left(1+\frac{1}{\gamma}\right)\frac{\partial^2 u'}{\partial y'^2} + g\beta_{T'}(T'-T'_\infty)\cos\alpha + g\beta_{C'}(C'-C'_\infty)\cos\alpha - \frac{\sigma B_0^2 u'}{\rho} - \frac{\mu\phi}{k'p}, \tag{1}$$

$$\frac{\partial v'}{\partial t'} + 2\Omega' u' = \frac{\partial^2 v'}{\partial y'^2} - \frac{\sigma B_0^2 u'}{\rho}, \tag{2}$$

$$\frac{\partial T}{\partial t'} = \frac{K_T}{\rho c_p}\frac{\partial^2 T'}{\partial y'^2} - \frac{1}{\rho c_p}\frac{\partial q_r}{\partial y'^2} + \frac{Q}{\rho c_p}(T'-T'_\infty), \tag{3}$$

$$\frac{\partial C'}{\partial t'} = Dm\frac{\partial^2 C'}{\partial y'^2}. \tag{4}$$

Under the initial and boundary conditions, we have

$$\left.\begin{aligned} &u' = 0,\ T' = T'_\infty,\ C' = C'_\infty, \text{ for all } y' \geq 0,\ t' \leq 0 \\ &u' = u_0 \cos wt,\ T' = T'_\infty + (T'_w - T'_\infty)\frac{t'}{t_0},\ C' = C'_\infty + (C'_w - C'_\infty)\frac{t'}{t_0} \\ &u' \to 0,\ T' \to T'_\infty,\ C' \to C'_\infty \text{ as } y' \to \infty \text{ and } t' \geq 0 \end{aligned}\right\}. \quad (5)$$

In the instance of an optically thin gray gas, the local radiant is presented with a Rosseland approximation:

$$\frac{\partial q'_r}{\partial y'} = -4a^*\sigma^*(T'^4_\infty - T'^4), \quad (6)$$

where σ^* indicates "the Stefan Boltzmann constant and a^* denotes the absorption coefficient correspondingly. Assuming that the temperature difference between the fluid within the boundary layer and the free stream is small, the term T'^4 can be approximated by a linear expression using a Taylor series expansion about the free stream temperature T'_∞. Expanding T'^4 in a Taylor series around T'_∞, and neglecting higher-order terms, we obtain

$$T'^4 \cong 4T'^3_\infty T' - 3T'^4_\infty. \quad (7)$$

This linearization simplifies the radiation term in the energy equation under the assumption of small temperature differences.

Substituting equations (6) and (7) in equation (3), we have

$$\rho C_p \frac{\partial T'}{\partial t'} = k\frac{\partial^2 T'}{\partial y^2} + 16a^*\sigma T'^3_\infty (T'_\infty - T'). \quad (8)$$

On suggesting the subsequent dimensionless quantities, we have

$$U = \frac{u'}{u_0},\ V = \frac{v'}{u_0},\ t = \frac{t'}{t_0},\ y = y'\frac{u_0}{u_0 t_0},\ \theta = \frac{T' - T'_\infty}{T'_w - T'_\infty},$$

$$C = \frac{C' - C'_\infty}{C'_w - C'_\infty},\ G_r = \frac{g\beta_{T'}(T'_w - T'_\infty)}{u_0^3},\ G_m = \frac{g\beta_{C'}(C'_w - C'_\infty)}{u_0^3},$$

$$M = \frac{\sigma B_0^2 \nu}{\rho u_0^2}, \quad P_r = \frac{\mu C_p}{k}, \quad S_c = \frac{v}{Dm}, \quad R = \frac{16\sigma^* T_\infty'^3}{k u_0^2},$$

$$\gamma = \frac{\mu_\beta \sqrt{(2\pi c)}}{p_y}, \quad Q = \frac{Q' v}{\rho c_p u_0^2}, \quad w = \frac{\omega \nu}{u_0^2}. \tag{9}$$

In expression $w = \frac{\omega \nu}{u_0^2}$,

w is the dimensionless frequency parameter,

ν is the kinematic viscosity of the fluid,

u_0^2 is the characteristic velocity amplitude of the oscillating plate,

ω is the angular frequency of oscillation.

3. Incorporating Laplace Transform Method

$$\frac{\partial U}{\partial t} - 2\Omega V = G_r \cos \alpha T + G_c \cos \alpha C + \left(1 + \frac{1}{\gamma}\right) \frac{\partial^2 U}{\partial y^2} - MU - \frac{1}{K} U, \tag{10}$$

$$\frac{\partial V}{\partial t} + 2\Omega U = \left(1 + \frac{1}{\gamma}\right) \frac{\partial^2 V}{\partial y^2} - MV, \tag{11}$$

$$\frac{\partial T}{\partial t} = \frac{1}{P_r} \frac{\partial^2 T}{\partial y^2} - RT + QT, \tag{12}$$

$$\frac{\partial C}{\partial t} = \frac{1}{S_c} \frac{\partial^2 C}{\partial y^2}. \tag{13}$$

Using the boundary condition and the pair of equations (10) and (11) together, we now exhibit a complex quickness, $q' = u + iv$, into a single equation (14):

$$\frac{\partial q'}{\partial t} = G_r \cos \alpha \theta + G_c \cos \alpha C + a \frac{\partial^2 q'}{\partial y^2} - mq', \tag{14}$$

$$\frac{\partial \theta}{\partial t} = \frac{1}{P_r}\frac{\partial^2 \theta}{\partial y^2} - R\theta + Q\theta, \tag{15}$$

$$\frac{\partial C}{\partial t} = \frac{1}{S_c}\frac{\partial^2 C}{\partial y^2}. \tag{16}$$

The following expressions represent the initial and boundary conditions in terms of the dimensionless variables:

$$q' = 0, \quad \theta = 0, \quad C = 0, \quad y \geq 0 \quad \text{and} \quad t \geq 0,$$

$$q' = \cos wt, \quad \theta = 1, \quad C = 1, \quad y = 0 \quad \text{and} \quad t > 0,$$

$$q' = 0, \quad \theta \to 0, \quad C \to 0, \quad y \to 0 \text{ as } y \to \infty \text{ and } t \geq 0, \tag{17}$$

here $m = M + 2i\Omega + \frac{1}{K}$ (it is meant for equation (14) only).

Explanation. m is a complex parameter that combines the effects of magnetic field strength (M), rotation (Ω), and the permeability of the porous medium (K) into a single term for simplified analysis using the Laplace transform method.

Equation (17) provides the dimensionless initial and boundary conditions that must be satisfied by the solution of equation (14).

4. Derived Solution

Equations (14)-(16) contain dimensionless administering conditions and corresponding beginning and limit conditions. These equations can be solved using Laplace transforms. After one last inverse transform, the following method is used to get the solutions:

$$q' = q_1 + q_2 + q_3 - q_4 - q_5, \tag{18}$$

$$q_1 = \begin{Bmatrix} \dfrac{e^{-iwt}}{2}\left[e^{-2\eta\sqrt{\frac{(m-iwa)t}{a}}}\, erfc\left(\dfrac{y}{2\sqrt{at}} - \sqrt{(m-iw)t}\right) + e^{2\eta\sqrt{\frac{(m-iwa)t}{a}}}\, erfc\left(\dfrac{y}{2\sqrt{at}} - \sqrt{(m-iw)t}\right)\right] \\ \dfrac{e^{iwt}}{2}\left[e^{-2\eta\sqrt{\frac{(m+iwa)t}{a}}}\, erfc\left(\dfrac{y}{2\sqrt{at}} - \sqrt{(m+iw)t}\right) + e^{2\eta\sqrt{\frac{(m-iwa)t}{a}}}\, erfc\left(\dfrac{y}{2\sqrt{at}} + \sqrt{(m+iw)t}\right)\right] \end{Bmatrix},$$

$$q_2 = \frac{G_r \cos\alpha}{b(1-aP_r)} \begin{Bmatrix} -\dfrac{e^{bt}}{2}\left[e^{-2\eta\sqrt{\left(\frac{m+b}{a}\right)t}}\, erfc\left(\dfrac{\eta}{\sqrt{a}} - \sqrt{\left(\frac{m+b}{a}\right)t}\right) + e^{2\eta\sqrt{\left(\frac{m+b}{a}\right)}}\, erfc\left(\dfrac{\eta}{\sqrt{a}} + \sqrt{\left(\frac{m+b}{a}\right)t}\right)\right] \\ +\dfrac{1}{2}\left[e^{-2\eta\sqrt{\frac{m}{a}t}}\, erfc\left(\dfrac{\eta}{\sqrt{a}} - \sqrt{\frac{m}{a}t}\right) + e^{2\eta\sqrt{\frac{m}{a}t}}\, erfc\left(\dfrac{\eta}{\sqrt{a}} + \sqrt{\frac{m}{a}t}\right)\right] \end{Bmatrix},$$

$$q_3 = \frac{G_m \cos\alpha}{c(1-aS_c)} \begin{Bmatrix} \dfrac{1}{2}\left[e^{-2\eta\sqrt{\frac{m}{a}t}}\, erfc\left(\dfrac{\eta}{\sqrt{a}} - \sqrt{\frac{m}{a}t}\right) + e^{2\eta\sqrt{\frac{m}{a}t}}\, erfc\left(\dfrac{\eta}{\sqrt{a}} + \sqrt{\frac{m}{a}t}\right)\right] \\ -\dfrac{e^{ct}}{2}\left[e^{-2\eta\sqrt{\left(\frac{m+c}{a}\right)t}}\, erfc\left(\dfrac{\eta}{\sqrt{a}} - \sqrt{\left(\frac{m+c}{a}\right)t}\right) + e^{2\eta\sqrt{\left(\frac{m+c}{a}\right)}}\, erfc\left(\dfrac{\eta}{\sqrt{a}} + \sqrt{\left(\frac{m+c}{a}\right)t}\right)\right] \end{Bmatrix},$$

$$q_4 = \frac{G_r \cos\alpha}{b(1-aP_r)}\left[\begin{array}{l}\frac{1}{2}\left[\begin{array}{l}e^{-2\eta\sqrt{P_r}\sqrt{(R-Q)t}}\,erfc(\eta\sqrt{P_r}-\sqrt{(R-Q)t}) \\ \quad + e^{2\eta\sqrt{P_r}\sqrt{(R-Q)t}}\,erfc(\eta\sqrt{P_r}+\sqrt{(R-Q)t})\end{array}\right] \\ +\frac{e^{bt}}{2}\left[\begin{array}{l}e^{-2\eta\sqrt{P_r}\sqrt{(R+b-Q)t}}\,erfc(\eta\sqrt{P_r}-\sqrt{(R+b-Q)t}) \\ \quad + e^{2\eta\sqrt{P_r}\sqrt{(R+b-Q)t}}\,erfc(\eta\sqrt{P_r}+\sqrt{(R+b-Q)t})\end{array}\right]\end{array}\right],$$

$$q_5 = \frac{G_m \cos\alpha}{c(1-aS_c)}\left\{erfc\,\eta\sqrt{S_c} - \frac{e^{ct}}{2}\left[\begin{array}{l}e^{-2\eta\sqrt{((S_c)c)t}}\,erfc(\eta\sqrt{S_c}-\sqrt{ct}) \\ \quad + e^{2\eta\sqrt{((S_c)c)t}}\,erfc(\eta\sqrt{S_c}+\sqrt{ct})\end{array}\right]\right\}, \tag{19}$$

$$\theta = \frac{1}{2}\left[\begin{array}{l}e^{-2\eta\sqrt{P_r}\sqrt{(R-Q)t}}\,erfc(\eta\sqrt{P_r}-\sqrt{(R-Q)t}) \\ \quad + e^{2\eta\sqrt{P_r}\sqrt{(R-Q)t}}\,erfc(\eta\sqrt{P_r}+\sqrt{(R-Q)t})\end{array}\right], \tag{20}$$

$$C = erfc(\eta\sqrt{S_c}). \tag{21}$$

5. Results and Interpretation

The numbers used in these simulations look at different physical properties in relation to the Grashof numbers for heat and mass transfer (G_r, G_c), the Schmidt number (S_c), time (t), the magnetic parameter (M), and the Soret number (S_r). The goal is to understand how the flow works by setting the Prandtl number (P_r) to 0.71, indicative of air. We have calculated the concentration, temperature, and velocity parameters for the selected parameters. Figure 3 shows the effects of the Prandtl number. It shows that as the Prandtl number rises up, the thickness of the thermal boundary layer declines, which makes the temperature distributions even more concentrated.

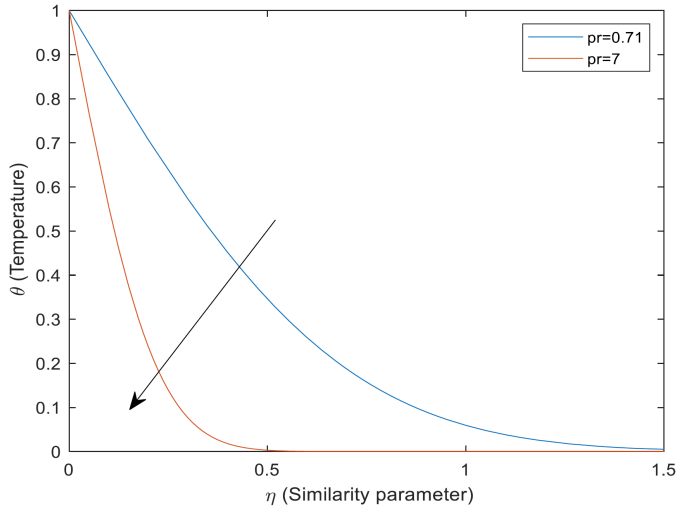

Figure 3. Temperature graph for various P_r values.

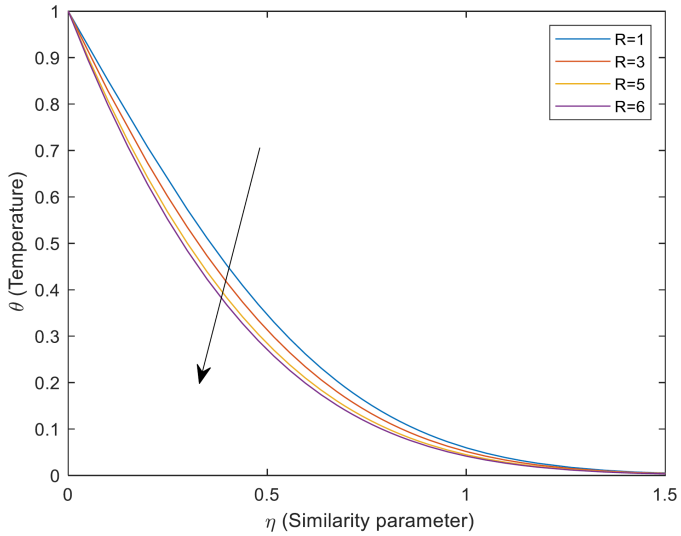

Figure 4. Profile of temperature for different R values.

A strong relationship between thermal radiation and temperature distribution is seen in Figure 4, which also shows how the radiation parameter affects temperature profiles. When the radiation parameter is reduced, the temperature rises, and when it is increased, the temperature

falls. This inverse connection states that high radiation levels effectively dissipate the fluid's thermal energy, causing the boundary layer temperature to drop.

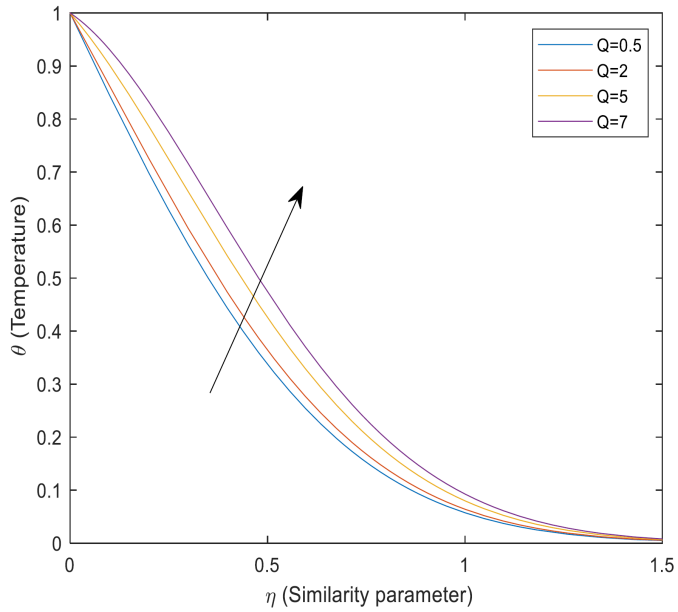

Figure 5. Profile of temperature for different values of Q.

Figure 5 illustrates the impact of the heat generation parameter on temperature profiles. There is a clear correlation between increasing the heat generation parameter and a corresponding rise in temperature, suggesting that the two are directly related to improving the thermal profile. This interaction proves that increasing the generation parameter causes the fluid's internal heat to rise, which in turn causes the boundary layer temperature to rise.

Figure 6 shows how concentration patterns are affected by the Schmidt number S_c. When S_c levels rise up, molecular diffusivity goes down and the concentration boundary layer gets thinner. This makes decrease in concentration. Therefore, lower S_c values correlate with greater species concentrations compared to higher S_c values.

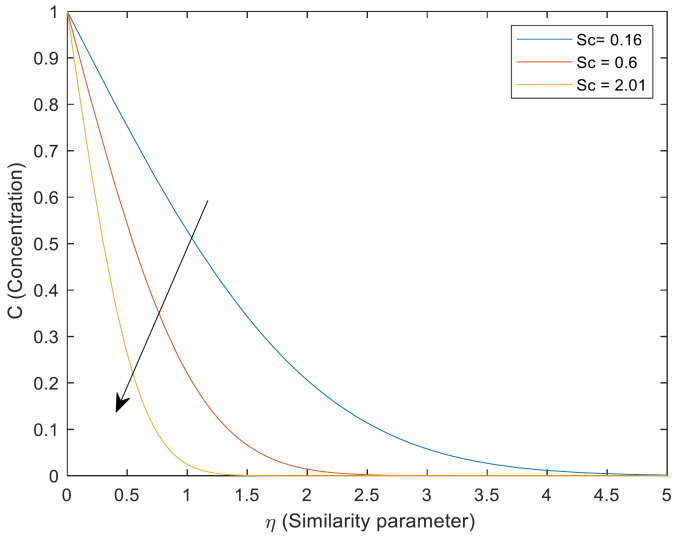

Figure 6. Profile of concentration for various S_c values.

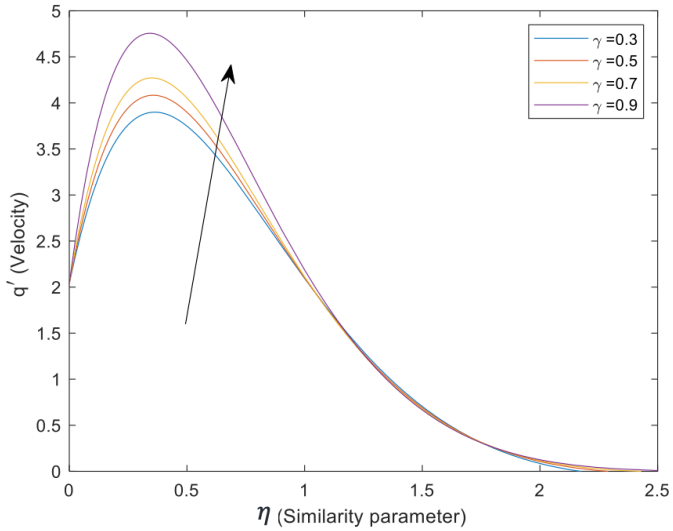

Figure 7. Profile of quickness for different γ values.

Figure 7 presents the variation in quickness profiles with respect to the Casson fluid parameter γ. Increasing γ notably enhances the quickness distribution within the boundary layer, with higher γ values leading to increased quickness profiles.

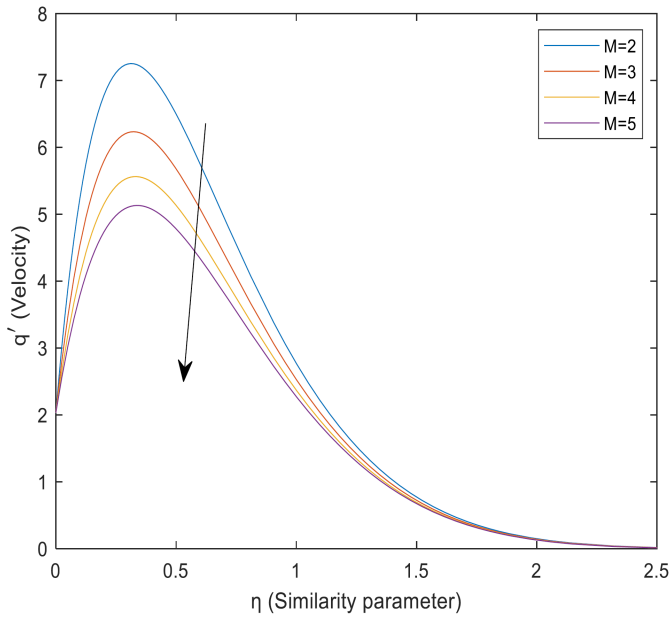

Figure 8. Profile of quickness for various *M* values.

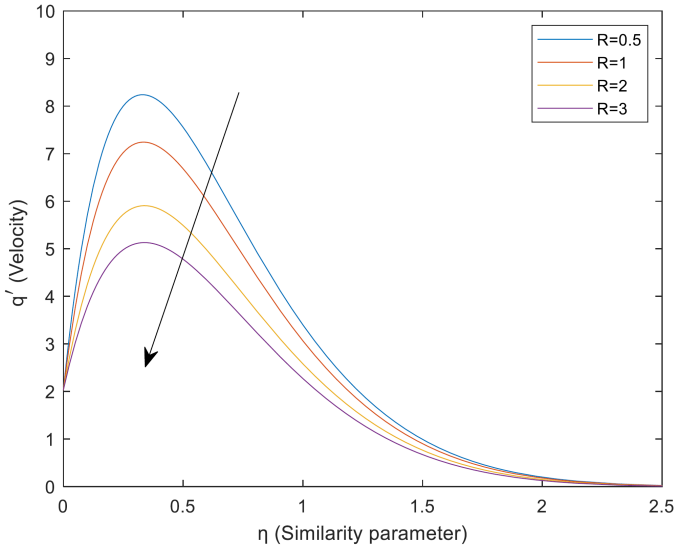

Figure 9. Profile of quickness for various values of *R*.

Figure 8 shows how the quickness profiles are affected by the magnetic parameter *M*. Generally, the fluid's mobility is reduced by the magnetic

field; this is demonstrated by the quickness graphs, which reveal a sharp decrease in the rate of transport with increasing magnetic parameter. Using a magnetic field, one may control the flow properties.

Figure 9 illustrates how the heating radiation number R influences the quickness profiles. It is possible to observe that when the heat thermal radiation parameter increments, the fluid quickness decreases.

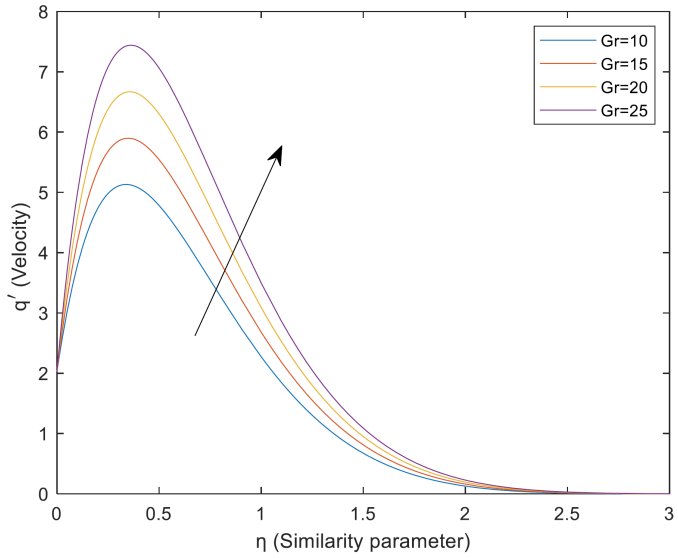

Figure 10. Profile of quickness for different G_r values.

Variation in quickness profiles as a function of Grashof number G_r is illustrated in Figure 10. As the Grashof number increases, the fluid quickness also growing forward. This happens because the buoyancy force grows, the boundary layer thickness and fluid quickness both rise, and the Grashof number has a higher value.

The quickness profiles are shown in Figure 11 as they fluctuate with mass Grashof number G_c. As the mass Grashof number increases, the fluid quickness likewise increases. This is because, as the mass Grashof number increases, the buoyancy force increases the fluid quickness and the boundary layer thickness.

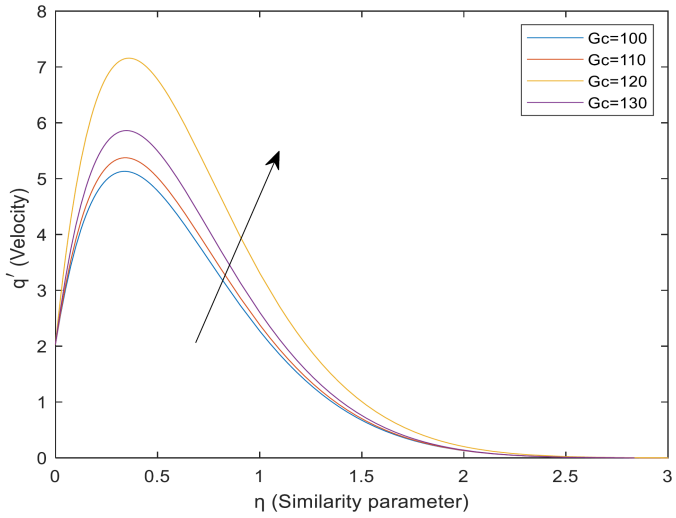

Figure 11. Profile of quickness for various G_c values.

Table 1. Profile comparison with the existing literature

Study/author	**Fluid type**	**Magnetic field** (M)	**Heat generation** (Q)	**Radiation** (R)	**Casson fluid parameter** (γ)	**Permeability** (K)	**Temperature profile**	**Concentration profile**	**Quickness profile**
Amar et al. [1]	Casson fluid	Yes	Yes	Yes	Yes	Yes	Increases with Q, decreases with R and P_r	Decreases with S_c	Decreases with M, S_c, R, P_r
Arthur et al. [2]	Casson fluid	Yes	Yes	Not specified	Yes	Yes	Not specified	Decreases with S_c	Decreases with M, S_c, P_r
Selvaraj and Jothi [3]	MHD flow	Yes	Yes	Yes	Not specified	Yes	Increases with Q, decreases with R and P_r	Increases with S_c	Increases with G_r, G_c, K
Bhavana et al. [4]	MHD flow	Yes	Not specified	Not specified	Not specified	Yes	Decreases with Q	Decreases with S_c	Decreases with M, S_c, P_r
Yanala et al. [5]	Casson fluid	Yes	Yes	Yes	Yes	Yes	Increases with Q, decreases with R and P_r	Decreases with S_c	Decreases with M, R, P_r
Kataria and Patel [9]	MHD flow	Yes	Yes	Yes	Not specified	Yes	Increases with Q, decreases with R, and P_r	Decreases with S_c	Decreases with M, S_c, R, P_r
Jamil et al. [11]	Casson fluid	Yes	Yes	Yes	Yes	Yes	Increases with Q, decreases with R and P_r	Decreases with S_c	Decreases with M, S_c, R, P_r

The findings from the comparison table correspond effectively with the title, elucidating the dynamic behavior of temperature, concentration, and quickness profiles under diverse conditions. The table indicates that heat generation (Q) markedly increases temperature, although thermal radiation (R) and the Prandtl number (P_r) diminish it, which is crucial to comprehending the interactions of thermal processes in an MHD Casson fluid. Concentration profiles are adversely influenced by the Schmidt number (S_c), which concurrently diminishes quickness, alongside the magnetic field (M) and thermal radiation (R). In contrast, the Casson fluid parameter (γ) and Grashof numbers (G_r, G_c) augment the quickness, which is crucial for comprehending fluid motion over an inclined oscillating plate. The permeability of the porous medium (K) facilitates fluid mobility, illustrating the complex interaction of magnetic fields, thermal radiation, heat generation, and fluid characteristics in this distinct MHD flow arrangement.

6. Conclusion

This work provides a comprehensive analysis of the effects of radiation, thermal generation, and oscillation on the unstable natural convection of Casson fluid over an infinite vertical plate in a rotating porous media under a uniform transverse magnetic field. The graphical depiction of focus, temperature, and speed profiles is affected by relevant parameters. Several notable findings emerge from the investigation:

- The temperature profile often increases over time in conjunction with the heat emission parameter Q, but the heat radiation parameter R and the Prandtl number P_r demonstrate an inverse correlation.

- The concentration boundary layer decreased as Schmidt's number increased. As the Schmidt number (S_c), magnetic parameter (M), radiation parameter (R), and Prandtl number (P_r) increase, the velocity decreases.

- In contrast, an elevation in the Casson fluid parameter γ, Grashof hydrothermal G_r, Grashof mass number G_c, and porous medium permeability K leads to an enhancement in velocity. The Casson fluid parameter γ is also increased.

This study elucidates the effects of radiation and thermal production on the magnetohydrodynamic Casson fluid flow in a porous media influenced by rotation on an inclined oscillating perpendicular plate; nevertheless, further investigation is necessary to explore the effects of varying boundary conditions. The study's findings offer substantial insights into the behavior of Casson fluid under various physical situations, facilitating the optimization of heat transfer processes in systems including rotating porous media, magnetic fields, and fluid convection. These discoveries have pragmatic applications for improving operations in industries requiring precise temperature and flow regulation, including chemical processing, energy systems, and materials engineering. We may strategically employ the modulation of heat production and magnetic field intensity to manage cooling in electronic systems or ensure thermal stability in polymer operations. The interaction of these factors at various initial and final conditions may enhance our design and management of magneto-convective flows in industrial applications, particularly in systems with complex geometries and significant temperature gradients. Examining alterations in boundary conditions may improve the applicability of these findings in other technical and environmental contexts.

Acknowledgement

The authors are highly grateful to the referee for his careful reading, valuable suggestions and comments, which helped to improve the presentation of this paper.

References

[1] N. Amar, N. Kishan and B. Shankar Goud, Viscous dissipation and radiation effects on MHD heat transfer flow of Casson fluid through a moving wedge with convective boundary condition in the existence of internal heat generation/absorption, Journal of Nanofluids 12(3) (2023), 643-651. https://doi.org/10.1166/jon.2023.1948.

[2] Emmanuel Maurice Arthur, Ibrahim Yakubu Seini and Letis Bortey Bortteir, Analysis of Casson fluid flow over a vertical porous surface with chemical reaction in the presence of magnetic field, Journal of Applied Mathematics and Physics 3(6) (2015), 713-723. http://dx.doi.org/10.4236/jamp.2015.36085.

[3] A. Selvaraj and E. Jothi, Heat source impacts on MHD and radiation absorption fluid flow past an exponentially accelerated vertical plate with exponentially variable temperature and mass diffusion through porous medium, Materials Today: Proceeding 46(9) (2021), 3490-3494. https://doi.org/10.1016/j.matpr.2020.11.919.

[4] M. Bhavana, D. Chenna Kesavaiah and A. Sudhakaraiah, The Soret effect on free convective unsteady MHD flow over a vertical plate with heat source, International Journal of Innovative Research Science Engineering and Technology 2(5) (2013), 1617-1628.

[5] Dharmendar Reddy Yanala, Bejawada Shankar Goud and Kottakkaran Sooppy Nisar, Influence of chemical reaction and heat generation/absorption on unsteady magneto Casson nanofluid flow past a non-linear stretching Riga plate with radiation, Case Studies in Thermal Engineering 50 (2023), 103494. https://doi.org/10.1016/j.csite.2023.103494.

[6] S. P. Devi and J. W. S. Anjali Raj, Thermo diffusion effects on unsteady hydromagnetic free convection flow with heat and mass transfer past a moving vertical plate with time dependent suction and heat source in a slip flow regime, Int. J. Appl. Math. and Mech. 7 (2011), 20-51.

[7] S. Dilip Jose and A. Selvaraj, Convective heat and mass transfer effects of rotation on parabolic flow past an accelerated isothermal vertical plate in the presence of chemical reaction of first order, JP Journal of Heat and Mass Transfer 24(1) (2021), 191-206. http://dx.doi.org/10.17654/HM024010191.

[8] D. Maran, A. Selvaraj, M. Usha and S. Dilip Jose, First order chemical response impact of MHD flow past an infinite vertical plate with in the sight of exponentially with variable mass diffusion and thermal radiation, Materials Today: Proceedings 46(9) (2021), 3302-3307. https://doi.org/10.1016/j.matpr.2020.11.464.

[9] Hari R. Kataria and Harshad R. Patel, Effects of chemical reaction and heat generation/absorption on magnetohydrodynamic (MHD) Casson fluid flow over an exponentially accelerated vertical plate embedded in porous medium with ramped wall temperature and ramped surface concentration, Propulsion and Power Research 8(1) (2019), 35-46. https://doi.org/10.1016/j.jppr.2018.12.001.

[10] J. Hartmann, Hg-dynamics I theory of the laminar flow of an electrically conductive liquid in a homogeneous magnetic field, Det. Kal. Dan. Vid. Sel. Mat. Medd. 15 (1937), 1-27. https://gymarkiv.sdu.dk/MFM/kdvs/mfm%2010-19/mfm-15-6.pdf.

[11] Dzuliana Fatin Jamil, Salah Uddin, Mohsin Kazi, Rozaini Roslan, M. R. Gorji and Mohd Kamalrulzaman Md Akhir, MHD blood flow effects of Casson fluid with Caputo-Fabrizio fractional derivatives through an inclined blood vessels with thermal radiation, Heliyon 9 (2023), e21780. https://doi.org/10.1016/j.heliyon.2023.e21780.

[12] Hari R. Kataria and Harshad R. Patel, Soret and heat generation effects on MHD Casson fluid flow past an oscillating vertical plate embedded through porous medium, Alexandria Engineering Journal 55(3) (2016), 2125-2137. https://doi.org/10.1016/j.aej.2016.06.024.

[13] J. L. McGregor, The application of the minimal energy hypothesis to a Casson fluid, The Bulletin of Mathematical Biophysics 32(2) (1970), 249-262. https://doi.org/10.1007/BF02476889.

[14] A. V. Mernone, J. N. Mazumdar and S. K. Lucas, A mathematical study of peristaltic transport of a Casson fluid, Math. Comput. Modelling 35(7-8) (2002), 895-912. https://doi.org/10.1016/S0895-7177(02)00065-7.

[15] S. Rama Mohan, G. Viswanatha Reddy and S. V. K. Varma, Dufour and radiation absorption effects on unsteady MHD free convection Casson fluid flow past an exponentially infinite vertical plate through porous medium, J. Emerging Technol. Innov. Res. 6 (2019), 485-512.

[16] C. Arruna Nandhini, S. Jothimani and Ali J. Chamkha, Combined effect of radiation absorption and exponential parameter on chemically reactive Casson fluid over an exponentially stretching sheet, Partial Differential Equations in Applied Mathematics 8 (2023), 100534. https://doi.org/10.1016/j.padiff.2023.100534.

[17] K. R. Raghunatha, Y. Vinod, Suma Nagendrappa Nagappanavar and Sangamesh, Unsteady Casson fluid flow on MHD with an internal heat source, Journal of Taibah University for Science 17(1) (2023), 2271691. https://doi.org/10.1080/16583655.2023.2271691.

[18] S. Dilip Jose and A. Selvaraj, Effects of parabolic flow past an accelerated isothermal vertical plate with heat and mass diffusion in the presence of rotation, Int. J. Aquatic Science 12(3) (2021), 256-263. https://doi.org/10.17654/hm024010191.

[19] A. Selvaraj, S. Dilip Jose, R. Muthucumaraswamy and S. Karthikeyan, MHD parabolic flow past an accelerated isothermal vertical plate with heat and mass diffusion in the presence of rotation, Materials Today: Proceedings 46(9) (2021), 3546-3549. https://doi.org/10.1016/j.matpr.2020.12.499.

[20] A. Sindhu, A. Selvaraj and S. Dilip Jose, Analysis on rotational impacts of parabolic flow past an accelerated isothermal vertical plate with variable temperature and uniform mass diffusion, Advances and Applications in Mathematical Sciences 21(11) (2022), 6373-6384. https://doi.org/10.1007/978-981-33-4389-4_38.

[21] E. Jothi, A. Selvaraj, S. Dilip Jose, A. Neel Armstrong and S. Karthikeyan, Effect of MHD and radiation absorption fluid flow past an exponentially accelerated vertical plate with variable temperature and concentration, S. L. Peng, R. X. Hao and S. Pal, eds., Proceedings of first International Conference on Mathematical Modelling and Computational Science, Advances in Intelligent Systems and Computing 1292 (2021), 429-439. https://doi.org/10.1007/978-981-33-4389-4_39.

[22] S. Dilip Jose, A. Selvaraj, R. Muthucumaraswamy, S. Karthikeyan and E. Jothi, MHD-parabolic flow past an accelerated isothermal vertical plate with variable temperature and uniform mass diffusion in the presence of rotation, S. L. Peng, R. X. Hao and S. Pal, eds., Proceedings of First International Conference on Mathematical Modelling and Computational Science, Advances in Intelligent Systems and Computing 1292 (2021), 417-428. https://doi.org/10.1007/978-981-33-4389-4_38.

[23] D. Lakshmikaanth, A. Selvaraj, L. Tamilselvi, S. D. Jose and V. Velukumar, Hall and heat source effects of flow state on a vertically accelerating plate in an isothermal environment, including chemical reactions, rotation, radiation, and the Dufour effect, JP Journal of Heat and Mass Transfer 37(4) (2024), 491-520. https://doi.org/10.17654/0973576324034.

[24] S. D. Jose, K. Selvaraj, P. N. Sudha, P. Geetha and D. Lakshmikaanth, Heat and mass transfer effects on parabolic flow past an accelerated isothermal vertical plate in the presence of chemical reaction and hall current, JP Journal of Heat and Mass Transfer 35 (2023), 55-74. https://doi.org/10.17654/0973576323042.

[25] D. Lakshmikaanth, A. Selvaraj, P. Selvaraju and S. D. Jose, Hall and heat source effects of flow past a parabolic accelerated isothermal vertical plate in the presence of chemical reaction and radiation, JP Journal of Heat and Mass Transfer 34 (2023), 105-126.

[26] M. Aruna, A. Selvaraj, S. Dilip Jose and S. Karthikeyan, Influence on MHD-parabolic flow across a vertical plate is triggered by a rotating fluid with uniform temperature and variable mass diffusion in the absence of Hall and Dufour effects, European Chemical Bulletin 12 (2023), 1123-1132.